

ORIGINAL RESEARCH

Tumor Necrosis Factor Alpha-Induced Protein-3 Inhibits the Activation of Hepatic Stellate Cells by Regulating the p65 Molecule in the NF- κ B Signaling Pathway

Hezhao Zhang, MD, Zhiyong Shi, MD, Yarong Guo, MD, Dongdong Wu, MS, Gao Yu, MS, Jun Xu, MD

ABSTRACT

Tumor necrosis factor alpha-induced protein-3, also called A20, is a zinc-finger protein that participates in various inflammatory responses; however, the putative relationship between A20 and hepatic fibrosis remains unelucidated. Therefore, we investigated the role and mechanism of action of A20 in activating hepatic stellate cells (HSC) during the progression of hepatic fibrosis. Cell counting kit-8 (CCK8), colony growth, transwell assays, cell cycle analysis, and apoptosis assays were performed to explore the effect of A20 on cell function in vitro. An interspecies intravenous injection of the adeno-associated virus was used to assess the in vivo role of A20. The regulation of A20 on p65 was detected using mass spectrometry and immunoprecipitation. Our findings revealed that A20 was

highly expressed in the liver tissues of patients with hepatic fibrosis and that the expression level of A20 in the liver tissue was closely correlated with the stage of liver fibrosis. In the LX-2 cell line, the downregulation of A20 upregulated the expression of fibrosis-related proteins and increased the expression of inflammatory factors, indicating the activation of HSC and vice versa. In addition, overexpression of A20 in mice reduced the degree of liver fibrosis in thioacetamide model mice. Finally, co-immunoprecipitation demonstrated that A20 could interact with p65. Hence, A20 inhibits HSC activation by binding to p65. (*Altern Ther Health Med*. [E-pub ahead of print.]

Hezhao Zhang, MD; Dongdong Wu, MS; Gao Yu, MS; Department: Faculty of Graduate Studies, Shanxi Medical University, Taiyuan, Shanxi, China. **Zhiyong Shi, MD; Yarong Guo, MD; Jun Xu, MD;** Department of Hepatopancreatobiliary Surgery, First Hospital of Shanxi Medical University, Taiyuan, Shanxi, China.

Corresponding author: Jun Xu, MD
E-mail: junxuty@163.com

INTRODUCTION

Hepatic fibrosis is a disease caused by imbalanced synthesis and degradation of the liver's extracellular matrix (ECM) after various pathological changes such as necrosis, apoptosis of hepatocytes, and inflammation. Abnormal deposition of fibrous connective tissue in the liver is a major phenotype of hepatic fibrosis during the pathological process.^{1,2} Owing to the lack of pathological diagnosis, the morbidity and mortality of liver fibrosis cannot be accurately estimated; however, in 2017, the number of patients with liver cirrhosis worldwide was estimated to be approximately 123 million, making it the 11th leading cause of death in the world, with 1.32 million deaths attributed to the disease.³ According to statistics,

approximately 7 million patients were affected with liver cirrhosis in China in 2015,⁴ and the number of related deaths in that year was approximately 160 000.⁵ Thus, liver fibrosis is relatively common in this population.

Various chronic liver diseases lead to liver cirrhosis and eventually to liver cancer, causing a high burden on society and families. The optimal treatment of liver fibrosis remains an urgent problem. A comprehensive study of the pathogenesis underlying liver fibrosis could provide novel insights into reversing and preventing the occurrence of liver cancer.

Hepatic stellate cells (HSC) are interstitial cells in the liver tissue. Under pathological conditions, HSC activates and transforms into myofibroblasts (MFB),^{6,7} Activated HSC enhances the expression of α -smooth muscle actin, forming fibroblasts and inflammatory molecules such as liver ECM. The gradual accumulation of ECM initiates the destruction of the physiological structure of the liver.^{8,9} Some studies have shown that the inhibition of HSC activation can significantly reduce liver injury and liver fibrosis.¹⁰ Nuclear factor κ B (NF- κ B) is a nuclear transcription factor that modulates various signal pathways and plays a vital role in the activation of HSC and the occurrence and development of hepatic fibrosis cirrhosis.¹¹⁻¹³ The NF- κ B transcription factor family consists of five different DNA-binding subunits, namely p65 (RelA),

c-rel (Rel), RelB, p105/p50 (NF- κ B1), and P100/p52 (NF- κ B2).¹⁴ NF- κ B p65 subunit is the central regulator of innate immunity. The anti-apoptotic function of p65 and the expression of tumor necrosis factor (TNF)- α -induced genes depend on the ability of p65 in binding and dimerization.¹⁵ Phosphorylation of p65 stimulates HSC activation, thus promoting the development of liver fibrosis.¹⁶

Dixit et al. first discovered the zinc-finger (ZnF) protein A20 in human umbilical vein endothelial cells.¹⁷ ZnF is a highly conserved metalloprotein with an amino-terminal tumor (OUT) domain at its N-terminus and seven zinc finger domains at its C terminal. The N-terminal thioacetamide domain mainly mediates deubiquitylation (DUB) activity. In the C-terminal domain, the ZnF4 and ZnF7 domains bind to the K63-linked ubiquitin (Ub) chain and M1-linked Ub chain, respectively, and support E3 Ub ligase activity.¹⁸ A20 can regulate the activation of NF- κ B and is also an inhibitor of pro-inflammatory signal pathways such as NF- κ B, c-Jun N-terminal kinase, extracellular signal-regulated kinase, and p38 mitogen-activated protein kinase pathways.¹⁹ In addition, A20 downregulates the NF- κ B signal pathway through Ub and then participates in cellular immunity, inflammation, hepatocyte proliferation, and apoptosis.²⁰ A20 exerts a protective effect on hepatocytes and participates in liver inflammation; however, its regulatory mechanism has not been elucidated.

In this study, we aimed to explore the role of A20 in hepatic inflammation and fibrosis. We observed low A20 expression in patients with hepatic fibrosis. Based on “gain of function” and “loss of function” strategies *in vitro* and *in vivo*, we revealed that A20 suppressed the invasion of HSC cell lines and liver fibrosis growth. In addition, co-immunoprecipitation (Co-IP) results showed that A20 directly interacted with p65. Therefore, our results confirm that A20 inhibits HSC activation by binding to p65.

MATERIALS AND METHODS

Patients

Fibrotic and healthy liver tissues were collected from the patients before any intervention. Liver tissue was collected from 100 patients. Among them, 81 patients had hepatic fibrosis (hepatitis B in 47 cases, hepatitis C in four cases, autoimmune hepatitis in five cases, primary biliary hepatitis in three cases, primary sclerosing cholangitis in two cases, alcoholic cirrhosis in nine cases, non-alcoholic fatty liver disease in two cases, drug-induced liver injury in two cases, cryptogenic cirrhosis in four cases, hepatolenticular degeneration in one case, and Budd-Chiari syndrome in two cases) and 19 patients had normal liver tissue (hepatic haemangioma in seven cases, hepatic cyst in nine cases, and hepatic rupture in three cases). Informed consent was obtained from all patients, and this study was approved by the Human Ethics Committee of First Hospital of Shanxi Medical University (NO.K096). The experiments were conducted according to the World Health Organization (WHO) criteria.

Flow cytometry

Flow cytometry detected A20 expression in peripheral blood mononuclear cells (PBMCs) obtained from 81 patients with chronic liver disease and 19 healthy volunteers.

Immunohistochemical (IHC) staining of HCC tissue microarray

First, the tissues were sliced using HE staining, and the target tissues were localized under a microscope with a mark on the paraffin. For each specimen, 3 target points were selected. A tissue microarray device was used to extract the paraffin columns (diameter 0.75 mm) from the original paraffin block. The columns were then inserted into the recipient paraffin block, from which the tissue microarray was eventually prepared. The obtained microarrays were all subjected to conventional section and HE staining. By referring to the user's guideline, Eli vision TM plus kit (Fuzhou Maxim Bio Co., Ltd. PR China) two-step technique was employed to carry out IHC staining, dewaxing, hydration, and antigen retrieval. The working concentration of anti-SMA, anti-FN, and anti-A20 was 1:500, 1:400 and, 1:200. Negative control sections were incubated with preimmune serum or with antiserum preabsorbed with a 100-fold excess of blocking peptide. PBS was substituted for the primary antibody to serve as the blank control. The sections underwent the DAB Color Development kit (Fuzhou Maxim Bio Co., Ltd. PR China) development and the development of hematoxylin.

Cell culture

The human HSC line LX-2 was originally obtained from the Cell Bank of the Chinese Academy of Sciences. The cells were cultured in RPMI-1640 medium (Hy clone) supplied with 10% fetal bovine serum (FBS; Gibco), 100 U/ml penicillin, and 100 mg/ml streptomycin (Gibco). All cells were maintained in an incubator at 37°C and 5% CO₂.

Cell proliferation assays

A cell proliferation reagent kit (cell counting kit-8 [CCK-8]) was used to determine the cell proliferation capacity of the liver fibrosis cell lines. Transfected cells were seeded in 96-well plates at a density of 5000 cells/well. According to the manufacturer's instructions, cell viability was assessed every 24, 48, 72, and 96 h.

Transwell assay

Transwell assays were performed to assess the invasion capacity of HSC cell lines under different treatments. Briefly, 1.0×10^4 cells in 200 μ l serum-free medium were plated into the upper chamber with a Matrigel-coated membrane (Corning Inc., USA), whereas 600- μ l medium supplemented with 10% FBS was added into the lower chamber. After 24 h of incubation at 37°C, the invaded cells were fixed with 20% methanol and stained with 0.1% crystal violet solution. Cells were visualized and imaged under a microscope in at least five random fields (Olympus, Japan).

Cell apoptosis assay

The transfected cells in early and late apoptosis stages were quantified with FITC-Annexin V. Briefly, the cells were collected and resuspended with 500- μ l binding buffer, followed by incubation with Annexin V in dark conditions for 15 minutes. The stained cells were analyzed using a BD FACS flow cytometer (BD Biosciences). The percentage of apoptotic cells was calculated and compared between different groups.

Cell cycle assay

Flow cytometric analysis was performed to examine DNA content after different treatments. The transfected cells were harvested and fixed with 75% pre-cold ethanol at -20°C overnight. The fixed cells were washed thrice with phosphate-buffered saline (PBS) and incubated with ribonuclease A at 37°C for 30 min. The cells were then stained with propidium iodide for 30 min at room temperature, and cell cycle profiles were determined by flow cytometry. The experiment was repeated independently at least thrice.

In vivo study

Forty clean grade C57BL/6 mice, 8 weeks old, male, weighing 20-25 g, were purchased from Beijing Weitong Lihua Experimental Animal Technology Co., Ltd. (Animal license number SCXK (Beijing) 2021-0006). The animals were kept at a temperature of 20-26 °C, in 40-70% humidity, and a 12/12 h light/dark cycle, with access to filtered water and food ad libitum. During the experiment, the body weight of mice was monitored at the same time every morning to evaluate the health status of mice. After one week of adaptation, 40 mice were randomly divided into four groups: (1) normal control group; (2) normal saline group, (3) thioacetamide (TAA) group, (4) TAA+A20 group. The TAA solution was prepared by dissolving 10 mg TAA in 1 ml of distilled water. The liver fibrosis model of TAA mice was established by intraperitoneal injection of the prepared TAA solution at a rate 0.1 ml per 10 g body weight. Pathological examination of the mouse liver was performed three weeks after TAA-induced liver fibrosis. If hyperplasia of the liver fibrous tissue, a small number of fibrous septa, and extensive hydroid changes in liver cells were observed, the hepatic fibrosis model was successfully established. In order to observe the expression of the virus, adeno-associated virus (AAV) virus containing green fluorescent protein purchased from Beijing Hesheng Biotechnology Co., Ltd. (3×10^{11} vg/ml) was injected into the mice through the tail vein, and the mice were killed three weeks later. In animal experiments, if mice exhibited persistent loss of appetite (weight loss of more than 20%), loss of mobility, severe organ or system damage (severe diarrhea, vomiting), progressive hypothermia, and other dying states, the experiment was suspended, and euthanasia was performed on the animals. One mouse in the TAA group died during the experiment, and the cause of death was related to poor individual tolerance to poisons. The other 39 mice reached the end of the experiment. Mice were euthanized with an overdose

of CO₂ gas with a CO₂ replacement rate of 20% of the cage volume per min (5 L/min), according to the AVMA Guidelines for Euthanasia. After CO₂ treatment, if the respiration and heartbeat stopped to prove the death of the mice, the liver was removed, and the animal diaphragm was cut to prevent resuscitation. Livers were removed and stored in a total freezer at -80°C for further analysis. Frozen sections of liver tissue were taken, and the expression of the virus was observed under a fluorescence microscope. After the stable expression of fluorescence, the expression time was observed, and the injection and experiment of no-load virus and overexpression A20 virus were carried out, as per the previously described method.

Histology assay

At the indicated time points, livers were harvested, formalin-preserved, embedded in paraffin, and processed to generate 5- μ m-thick sections. Masson-stained sections were examined to assess inflammatory infiltrate and the degree of fibrosis. Pathological sections of liver tissue were observed under an Olympus-positive microscope. The Aperio analysis algorithm in the ImageScope12.4.3 image analysis system was used to measure the proportion area of collagen in the visual field for semi-quantitative analysis of liver fibrosis. Five non-overlapping visual fields in the portal area were randomly selected for observation and statistical analyses.

Co-IP assay

Transfected cells were lysed with radioimmunoprecipitation assay lysis buffer and prepared for the Co-IP assay. After incubating protein A/G beads with the primary antibody or IgG at 4°C for 6–8 h, the prepared cell lysate was added to the mixture of beads and antibody overnight at 4°C. The mixture was washed three times with PBS containing 0.1% NP40 and eluted using an elution buffer. Finally, the eluted samples were analyzed using SDS-PAGE, silver staining (Beyotime, China), and mass spectrometry.

Western blot assay

For western blot assays, HSCs were harvested in the lysis buffer. The total protein concentration was evaluated using a bicinchoninic acid (BCA) protein assay kit (Thermo Fisher Scientific, Inc.). The proteins were then separated by 12% SDS-PAGE and transferred onto PVDF membranes (Thermo Fisher Scientific, Inc.). After incubation with 5% milk at room temperature for 1 h, the membranes were maintained with primary antibody as indicated at 4°C overnight and then incubated with secondary antibodies at room temperature for 1.5 h. Protein bands were visualized with an enhanced chemiluminescence (ECL) assay (Millipore, Billerica, MA, USA). Glyceraldehyde 3-phosphate dehydrogenase (GAPDH) acted as an endogenous control. The primary antibodies used were as follows: anti-GAPDH (60004-1-IG, Proteintech), anti-Fibronectin (15613-1-ap, Proteintech), anti- α -SMA (19245, CST), and anti-A20 (66695-1-IG, Proteintech).

Table 1. qRT-PCR primers for the detected genes.

	forward,	reverse
siCtrl	5'-CAGUACUUUUGUGUAGUACAAA-3'	5'-UUCUCCGAACGUGUCACGUTT-3'
siA20#1	5'-GCACCAUGUUUGAAGGAUAAdTdT-3'	5'UAUCUCAAACAUGGUGCdTdT-3'
siA20#2	5'-CAAAGUUGGAUGAAGCUAAdTdT-3'	5'-UUAGCUUCAUCCAACUUUGdTdT-3'
siA20#3	5'-CACUGGAAGAAUACACAUAdTdT-3'	5'-AUAUGUUAUUUCUCCAGUGdTdT-3'
GAPDH	5'-ACAACCTTGGTATCGTGAAGG-3'	5'-GCCATCACGCCACAGTTTC-3'
A20	5'-TCCTCAGGCTTTGATTGAGC-3'	5'-TGTGTATCGGTGCATGG TTTTA-3'
α -SMA	5'-AAAAGACAGCTACGT GGGTGA-3'	5'-GCCATGTCTATCGGGTACTTC-3'
FN	5'-CGGTGGTGTCTAGTCAAAG-3'	5'-AAACCTCGGCTTCTCCATA A-3'

Figure 1. A20 is downregulated in human hepatic fibrosis patients. **A.** The expression of A20 in the peripheral blood of 81 patients with chronic liver disease and 19 volunteers was detected using flow cytometry, $P < .01$. **B.** Immunohistochemical detection of the expression of A20 in fibrotic liver tissue showed that the expression level of A20 increased with the aggravation of fibrosis, and a significant difference was observed between S0 and S1–S4; S1 and S3; S4, S2, S3, and S4, $P < .05$.

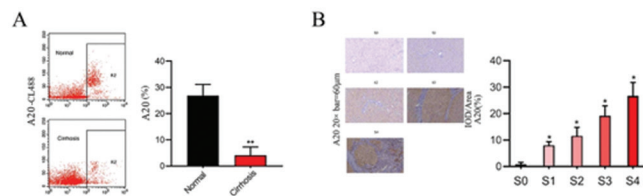
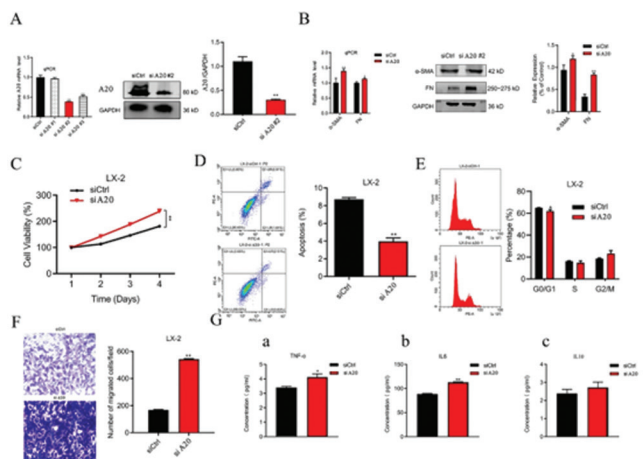


Figure 2. Decreasing the expression of A20 upregulates the expression of fibrosis-related proteins and inflammatory factors and activates hepatic stellate cells. **A.** qPCR and western blot were used to detect the expression of A20 in indicated LX-2 cells. **B.** qPCR and western blot detection of indicated genes' expression in siCtrl and siA20#2 cells (** $P < .01$, vs siCtrl). **C.** The effect of siRNA or siCtrl on the proliferation of A20-silenced LX-2 cells was detected by CCK-8 assay (** $P < .01$, vs siCtrl). **D.** Detection of apoptosis rate by flow cytometry. **E.** Detection of cell cycle progression of LX-2 cells by flow cytometry. **F.** Transwell assay was used to detect the effects of A20 and siCtrl on LX-2 cell invasion (** $P < .01$, vs siCtrl). **G.** ELISA was used to detect the secretion of inflammatory factors TNF- α , IL6, and IL10 in the supernatant of LX-2 culture medium after knocking down the expression of A20 (* $P < .05$, vs siCtrl; ** $P < .01$, vs siCtrl).



Quantitative reverse transcription-polymerase chain reaction (qRT-PCR) assay

The qRT-PCR was performed according to previously described protocols. Quantitative PCR primer sequences were shown in Table 1

Transfection protocol

LX-2 cells were inoculated into a 6-well plate with $40 \sim 60 \times 10^4$ cells per well and 2 compound pores. Cell transfection was performed when the cell growth covered more than 60% of the petri dish. The plasmids of each group were diluted to 4nM with 1 640 medium, respectively. Then, 6 μ l Lipo2000 was diluted to 20 μ l, and the plasmid containing Lipo2000 was mixed with 1640 after incubation for 15 min and incubated for 20 min. After the cells were replaced with a new medium, a mixture of 40 μ l was added to each well. Cultured at 37°C in a 5% CO₂ cell incubator for 48 h; 48 h after transfection, the cells were examined under a fluorescence microscope, and the qualified cells were subjected to follow-up experiments.

Statistical analyses

The corresponding experimental results were analyzed using SPSS (22.0) statistical software. The results were presented as mean \pm standard deviation ($\bar{x} \pm s$). Differences between multiple groups were compared using a one-way analysis of variance, followed by Tukey's multiple comparison test. The parameters were set at $\alpha = 0.05$ and $P < .05$.

RESULTS

A20 is lowly expressed in the peripheral blood of human hepatic fibrosis patients

First, we studied the expression of A20 in the peripheral blood and liver tissues of 19 healthy volunteers and 81 patients with fibrosis. Flow cytometry results showed that the expression of A20 in the peripheral blood was lower in the fibrotic group (Figure 1A). Next, we subjected fibrotic livers at different stages to immunohistochemical staining for A20. As a result (we divided liver fibrosis into S0–S4 stages based on the METAVIR system: S0=no fibrosis, S1=portal fibrosis without septa, S2=portal fibrosis with rare septa, S3=numerous septa without cirrhosis, and S4=cirrhosis), A20 expression gradually increased in the fibrotic liver tissues to a higher degree (Figure 1B).

Downregulation of A20 upregulates the expression of fibrosis-related proteins and inflammatory factors and activates hepatic stellate cells

To determine the role of A20 in liver fibrosis, we transfected LX-2 cells with siRNAs against the negative control and A20. The results showed that A20 protein expression significantly decreased after transfection with siA20#2 (Figure 2A). Thus, we selected siA20#2 for follow-up experiments. We also observed that A20 knockdown increased the expression of α -SMA and FN (Figure 2B), indicating that its downregulation significantly activated the HSCs. Furthermore, CCK-8 assay

confirmed that A20 knockdown significantly promoted the proliferation of LX-2 cells (Figure 2C). The apoptosis rate was decreased in the A20 knockdown group than that in the control group (Figure 2D). Cell cycle progression was detected using flow cytometry. The results showed that the proportion of LX-2 cells in the G0/G1 phase decreased significantly. In contrast, those in the S phase increased significantly after A20 knockdown (Fig.2E). Through the transwell experiment in the LX-2 cell line, the migration ability of A20 knockout cells was significantly enhanced compared with that of control cells (Figure 2F). Enzyme-linked immunosorbent assay (ELISA) was used to detect the secretion of inflammatory cytokines, including TNF- α , interleukin (IL) 6 and IL10, in the supernatant of LX-2 culture medium. The results showed that A20 knockdown promoted the secretion of TNF- α and IL6 but not IL-10 (Figure 2G). These data suggest that A20 can regulate the cellular processes of LX-2 cells, including cell proliferation, invasion, cell cycle, apoptosis, and inflammatory response.

Overexpression of A20 inhibits the expression of liver fibrosis-related proteins and inflammatory factors and inactivates hepatic stellate cells.

To confirm the role of A20 in the occurrence and development of hepatic fibrosis, a plasmid containing A20 was transferred into LX-2 cells to overexpress A20 (Figure 3A). Changes in HSC activation and fibrosis-related indices were detected after A20 overexpression. Compared with the wild type, the mRNA expression of α -SMA and FN decreased. Correspondingly, the expression of α -SMA (protein of gene α -SMA) and FN was also decreased at the protein level, as demonstrated using western blotting (Figure 3B), indicating that the degree of cell fibrosis decreases after overexpression of A20. The results of the CCK-8 and colony formation assays showed that overexpression of A20 inhibited cell proliferation and colony formation (Figure 3C). Compared to the control group, the apoptosis rate in the A20 overexpression group was significantly increased (Figure 3D). In addition, the proportion of LX-2 cells in G0/G1 phase increased significantly, whereas that of cells in S phase decreased significantly after A20 overexpression (Figure 3E). The migratory ability of cells was significantly weakened after A20 overexpression (Figure 3F). The abundance of TNF- α and IL6 was reduced, whereas that of IL10 was slightly enhanced in the supernatant of LX-2 culture medium after overexpression of A20 (Figure 3G). Thus, the overexpression of A20 had a function opposite to that of A20 knockdown.

Effect of A20 on hepatic fibrosis development in TAA model mice

To further study the effect of A20 upregulation on the progression of hepatic fibrosis in mice, TAA was used to induce liver fibrosis (Figure 4A). Three weeks later, pathological examination of the liver of mice showed hyperplasia of fibrous tissue, formation of a small number of fibrous septa, and extensive watery changes of hepatocytes, confirming liver fibrosis. The virus was injected into mice

Figure 3. Overexpression of A20 inhibits the expression of liver fibrosis-related proteins and inflammatory factors and inactivates hepatic stellate cells. **A.** qPCR and western blot were used to detect the expression of A20 in the LX-2 cell line transfected with plasmid and the expression of A20. **B.** qPCR and western blot detection of indicated genes after A20 overexpression (***P* < .01, vs Ctrl). **C.** CCK-8 assay was used to detect the effect of Ctrl and A20 overexpression on the proliferation of LX-2 cells (***P* < .01, vs siCtrl). **D.** Detection of apoptosis rate by flow cytometry. **E.** Detection of cell cycle distribution by flow cytometry. **F.** Transwell method was used to detect the effects of A20 on LX-2 cell invasion (***P* < .01, vs siCtrl). **G.** ELISA was used to detect the secretion of inflammatory factors TNF- α , IL6, and IL10 in the supernatant of LX-2 culture medium after overexpression of A20 (**P* < .05, ***P* < .01, vs Ctrl).

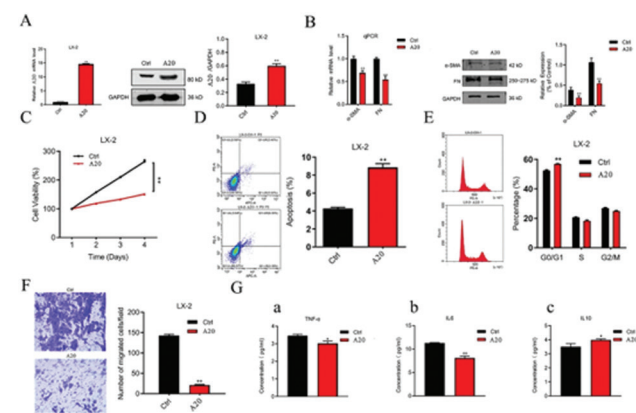
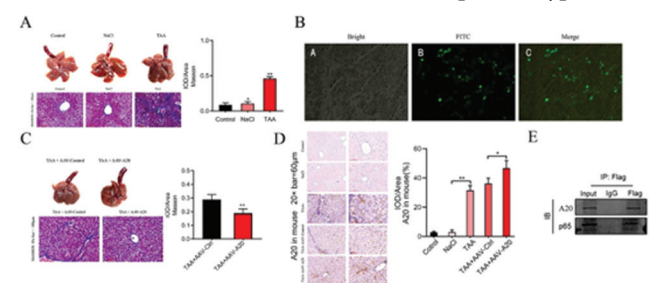


Figure 4. Effect of A20 on hepatic fibrosis degree in TAA model mice. **A.** TAA-induced liver fibrosis in mice. Three weeks later, the mice were killed and photographed, and the liver tissues of the mice were stained with Masson (***P* < .01, vs Ctrl). **B.** Fluorescence microscopy confirmed that the virus was stably expressed in liver tissue. **C.** The virus was injected into the mice through the tail vein. Three weeks later, the mice were killed and photographed, and the liver tissues of the mice were stained with Masson (***P* < .01, vs TAA+AAV-Ctrl). **D.** Expression of A20 protein in mouse liver tissue (***P* < .01, vs. NaCl; **P* < .05, vs. TAA+AAV-Ctrl). **E.** Co-immunoprecipitation results indicate that A20 could bind to the p65 subtype.



through the tail vein to establish a model of A20 overexpression. Fluorescent spots were observed under a fluorescence microscope in the liver tissue of mice injected with the virus, indicating that the virus was stably expressed in the liver tissue (Figure 4B). Compared to the liver tissue of

TAA mice transfected with A20, the expression of A20 increased after virus injection and hepatic fibrosis was alleviated, as shown by Masson staining (Figure 4C and D). These results suggest that the expression of A20 inhibits the progression of liver fibrosis, which is consistent with the results of the *in vitro* studies.

A20 contributes to the activation of hepatic stellate cells by regulating p65 expression

The signaling pathways regulated by A20 in HSC (Table 1) have been previously reported. The results of Co-IP showed that A20 might inhibit HSC activation by binding to p65 (Figure 4E).

DISCUSSION

Hepatic fibrosis is a self-repairing reaction of liver tissue after injury and occurs in the early stage of liver cirrhosis.²¹ HSC activation is a major risk factor for hepatic fibrosis. Excessive activation of HSC induces enhanced ECM deposition in the liver, leading to hepatic fibrosis.²² NF- κ B is the critical factor in regulating hepatocyte inflammation, and the activation of HSC is regulated by NF- κ B.²³ A20 is an effective anti-inflammatory agent. Mutations of gene encoding A20 are associated with a series of inflammatory pathologies in humans and mice. A20 exerts anti-inflammatory effects by inhibiting NF- κ B signal transduction via Ub.²⁰ A20 is involved in initiating and developing hepatic fibrosis; however, the specific mechanism requires further exploration.

The expression of A20 in the peripheral blood of patients with hepatic fibrosis and its significance as a marker of hepatic fibrosis have not been reported. Thus, we investigated the role and mechanism of A20 in HSC activation and clarified its role in hepatic fibrosis. Flow cytometry analysis revealed that the level of A20 protein in the peripheral blood of patients with hepatic fibrosis was significantly lower than that in healthy participants, indicating that A20 is related to the occurrence and development of hepatic fibrosis and may be a protective factor against the development of hepatic fibrosis.

To further explore the role of A20 in hepatic fibrosis, we used immunohistochemistry to detect the expression levels of A20 in liver tissue samples at different stages of hepatic fibrosis. α -SMA is involved in wound contraction and scar formation and can synthesize FN involved in fibroblast differentiation, which is essential for fibrosis development. The results showed that A20 was marginally expressed in the cytoplasm of normal hepatocytes, which is consistent with previous studies (the expression level of A20 in normal tissues was low).²⁴ In patients with hepatic fibrosis, the expression level of A20 increased significantly, and interestingly, the expression level of A20 increased with the increase in the degree of hepatic fibrosis. The expression site gradually expanded from the hepatocytes and inflammatory necrotic areas to the hepatic sinusoid wall, vascular fibrosis septum, and other tissues. The above phenomena do not seem consistent with the expression of A20 in peripheral

blood. However, some studies have shown that A20 can also be induced by pro-inflammatory factors and mitogens.²⁵ Combined with the above experimental phenomena, A20 may be induced by inflammatory factors in liver cells, and the ability of A20 expression differs in different fibrotic pathological processes of hepatocytes; however, the specific mechanism remains to be further studied.

To further investigate the precise role of A20 in the development of liver fibrosis, we altered the expression of A20 in LX-2 cells. We found that A20 inhibited the expression of HSC activation biomarkers. Furthermore, by injecting the overexpressed A20 virus vector into the tail vein of mice, we overexpressed A20 in TAA model mice and observed that the level of liver fibrosis was improved. At the cellular and *in vivo* levels, we found that A20 plays a vital role in the activation of HSC and participation in hepatic fibrosis. However, the mechanism by which A20 regulates HSC and affects hepatic fibrosis is not precise.

Some studies have shown that hepatocyte-specific A20 gene knockout mice are highly sensitive to hepatocyte apoptosis, chronic hepatitis, and hepatocellular carcinoma, which are involved in the NF- κ B signaling pathway.²⁶⁻²⁸ Other studies have shown that overexpression of A20 inactivates the NF- κ B signal pathway by various mechanisms.²⁹⁻³¹ This further suggests that A20 may target the upstream receptor proximal molecules to inhibit NF- κ B signal transduction. We previously found that the overexpression of A20 improved the degradation and apoptosis of chondrocytes *in vitro* by inhibiting the activity of p65, thus reducing inflammation in osteoarthritis mice.³² In addition, a study on the hepatotoxicity of trovafloxacin (TVX) found that the prolongation of p65 translocation induced by TVX was related to the accumulation of A20 during the inducing hepatocyte apoptosis.³³ A20 is suggested to be involved in regulating p65 in the NF- κ B family in liver inflammation. In this study, we performed immunoprecipitation and mass spectrometry to screen and detect the proteins that bind to A20. The results showed that the downstream molecule binding to A20 was p65, a molecule of the NF- κ B family. We conclude that A20 may inhibit HSC activation by binding to p65.

CONCLUSION

In summary, our study demonstrates the key role of A20 in the proliferation, invasion, cell cycle, and apoptosis in liver fibrosis. We demonstrated that A20 combined with p65 and confirmed its role in liver fibrosis by knocking down or overexpressing A20 in LX-2 cells. Our findings suggest that A20 is a promising target for preventing hepatic fibrosis and fibrosis-related diseases.

ACKNOWLEDGMENTS

We thank Wenhao Shao for assistance with the experiments and Fanxiu Meng for valuable discussions.

FUNDING

This work was supported by the Natural Science Foundation of the Health Commission of Shanxi Province (grant numbers 2020TD08, 2020085, 201901D211516, and 2020090).

AVAILABILITY OF DATA AND MATERIALS

The data generated in the present study may be requested from the corresponding author.

AUTHORS' CONTRIBUTIONS

Hezhao Zhang and Zhiyong Shi contributed equally to the work.

ETHICS APPROVAL AND CONSENT TO PARTICIPATE

This study was performed in accordance with the principles of the Declaration of Helsinki. This study was approved by the Ethics Committee of Shanxi Medical University (6 September 2021; No. K097). Written informed consent was obtained from patients and their guardians who participated in the study. The experimental design, experimental process, and animal killing method were reviewed by the Experimental Animal Welfare Ethics Review Committee of Shanxi Medical University and met the requirements of animal ethics and animal welfare; The Ethics number is SYXK(Shanxi)2019-0007.

COMPETING INTERESTS

The authors declare that they have no competing interests.

REFERENCES

1. Kisseleva T, Brenner DA. Fibrogenesis of parenchymal organs. *Proc Am Thorac Soc*. 2008;5(3):338-342. doi:10.1513/pats.200711-168DR
2. Friedman SL. Mechanisms of hepatic fibrogenesis. *Gastroenterology*. 2008;134(6):1655-1669. doi:10.1053/j.gastro.2008.03.003
3. Sepanlou SG, Safiri S, Bisignano C, et al; GBD 2017 Cirrhosis Collaborators. The global, regional, and national burden of cirrhosis by cause in 195 countries and territories, 1990-2017: a systematic analysis for the Global Burden of Disease Study 2017. *Lancet Gastroenterol Hepatol*. 2020;5(3):245-266. doi:10.1016/S2468-1253(19)30349-8
4. Xiao J, Wang F, Wong NK, et al. Global liver disease burdens and research trends: analysis from a Chinese perspective. *J Hepatol*. 2019;71(1):212-221. doi:10.1016/j.jhep.2019.03.004
5. Sarin SK, Kumar M, Eslam M, et al. Liver diseases in the Asia-Pacific region: a Lancet Gastroenterology & Hepatology Commission. *Lancet Gastroenterol Hepatol*. 2020;5(2):167-228. doi:10.1016/S2468-1253(19)30342-5
6. Yan Y, Zeng J, Xing L, Li C. Extra- and Intra-Cellular Mechanisms of Hepatic Stellate Cell Activation. *Biomedicines*. 2021;9(8):1014. doi:10.3390/biomedicines9081014
7. Krizhanovsky V, Yon M, Dickens RA, et al. Senescence of activated stellate cells limits liver fibrosis. *Cell*. 2008;134(4):657-667. doi:10.1016/j.cell.2008.06.049
8. Chen RJ, Wu HH, Wang YJ. Strategies to prevent and reverse liver fibrosis in humans and laboratory animals. *Arch Toxicol*. 2015;89(10):1727-1750. doi:10.1007/s00204-015-1525-6
9. Novo E, Cannito S, Morello E, et al. Hepatic myofibroblasts and fibrogenic progression of chronic liver diseases. *Histol Histopathol*. 2015;30(9):1011-1032.
10. Puche JE, Lee YA, Jiao J, et al. A novel murine model to deplete hepatic stellate cells uncovers their role in amplifying liver damage in mice. *Hepatology*. 2013;57(1):339-350. doi:10.1002/hep.26053
11. Nikolaou K, Tsagaratou A, Eftychi C, Kollias G, Mosialos G, Talianidis I. Inactivation of the deubiquitinase CYLD in hepatocytes causes apoptosis, inflammation, fibrosis, and cancer. *Cancer Cell*. 2012;21(6):738-750. doi:10.1016/j.ccr.2012.04.026
12. Kelly C, Williams MT, Mitchell K, Elborn JS, Ennis M, Schock BC. Expression of the nuclear factor- κ B inhibitor A20 is altered in the cystic fibrosis epithelium. *Eur Respir J*. 2013;41(6):1315-1323. doi:10.1183/09031936.00032412
13. Treiber M, Neuhofer P. Myeloid, but not pancreatic, RelA/p65 is required for fibrosis in a mouse model of chronic pancreatitis. *Gastroenterology*. 2011; 141(4):1473-1485. doi:10.1053/j.gastro.2011.04.026
14. Taniguchi K, Karin M. NF- κ B, inflammation, immunity and cancer: coming of age. *Nat Rev Immunol*. 2018;18(5):309-324. doi:10.1038/nri.2017.142
15. Riedlinger T, Liefke R, Meier-Soelch J, et al. NF- κ B p65 dimerization and DNA-binding is important for inflammatory gene expression. *FASEB J*. 2019;33(3):4188-4202. doi:10.1096/fj.201801638R
16. Wang K, Fang S. TGF- β 1/p65/MAT2A pathway regulates liver fibrogenesis via intracellular SAM. *EBioMedicine*. 2019; 42:458-469
17. Varani J, Dame MK, Taylor CG, et al. Age-dependent injury in human umbilical vein endothelial cells: relationship to apoptosis and correlation with a lack of A20 expression. *Lab Invest*. 1995;73(6):851-858.
18. Lu TT, Onizawa M, Hammer GE, et al. Dimerization and ubiquitin mediated recruitment of A20, a complex deubiquitinating enzyme. *Immunity*. 2013;38(5):896-905. doi:10.1016/j.immuni.2013.03.008
19. Wu Y, He X, Huang N, Yu J, Shao B. A20: a master regulator of arthritis. *Arthritis Res Ther*. 2020;22(1):220. doi:10.1186/s13075-020-02281-1
20. Priem D, van Loo G, Bertrand MJM. A20 and Cell Death-driven Inflammation. *Trends Immunol*. 2020;41(5):421-435. doi:10.1016/j.it.2020.03.001
21. Ahmed H, Umar MI. TGF- β 1 signaling can worsen NAFLD with liver fibrosis backdrop. *Exp Mol Pathol*. 2022; 124:104733
22. Yu Q, Cheng P, Wu J, Guo C. PPAR γ /NF- κ B and TGF- β 1/Smad pathway are involved in the anti-fibrotic effects of levo-tetrahydropalmatine on liver fibrosis. *J Cell Mol Med*. 2021;25(3):1645-1660. doi:10.1111/jcmm.16267
23. Luedde T, Schwabe RF. NF- κ B in the liver—linking injury, fibrosis and hepatocellular carcinoma. *Nat Rev Gastroenterol Hepatol*. 2011;8(2):108-118. doi:10.1038/nrgastro.2010.213
24. Verstrepen L, Verhelst K, van Loo G, Carpentier I, Ley SC, Beyaert R. Expression, biological activities and mechanisms of action of A20 (TNFAIP3). *Biochem Pharmacol*. 2010;80(12):2009-2020. doi:10.1016/j.bcp.2010.06.044
25. Chen H, Wu X, Zhou H, He Z, Li H, Wang Q. Epidermal growth factor upregulates the expression of A20 in hepatic cells via the MEK1/MSK1/p-p65 (Ser276) signaling pathway. *Am J Transl Res*. 2021;13(2):708-718.
26. Martens A, Van Loo G. A20 at the Crossroads of Cell Death, Inflammation, and Autoimmunity. *Cold Spring Harb Perspect Biol*. 2020;12(1).
27. Catrysse L, Vereecke L, Beyaert R, van Loo G. A20 in inflammation and autoimmunity. *Trends Immunol*. 2014;35(1):22-31. doi:10.1016/j.it.2013.10.005
28. de Boer YS, van Gerven NM, Zwiers A, et al; Dutch Autoimmune Hepatitis Study Group; LifeLines Cohort Study; Study of Health in Pomerania. Genome-wide association study identifies variants associated with autoimmune hepatitis type 1. *Gastroenterology*. 2014;147(2):443-52.e5. doi:10.1053/j.gastro.2014.04.022
29. Song HY, Rothe M, Goeddel DV. The tumor necrosis factor-inducible zinc finger protein A20 interacts with TRAF1/TRAF2 and inhibits NF- κ B activation. *Proc Natl Acad Sci USA*. 1996;93(13):6721-6725. doi:10.1073/pnas.93.13.6721
30. Jäättelä M, Mouritzen H, Elling F, Bastholm L. A20 zinc finger protein inhibits TNF and IL-1 signaling. *J Immunol*. 1996;156(3):1166-1173. doi:10.4049/jimmunol.156.3.1166
31. Heyninck K, Beyaert R. The cytokine-inducible zinc finger protein A20 inhibits IL-1-induced NF- κ B activation at the level of TRAF6. *FEBS Lett*. 1999;442(2-3):147-150. doi:10.1016/S0014-5793(98)01645-7

32. Cui SB, Wang TX, Liu ZW, Yan JY, Zhang K. Zinc finger protein A20 regulates the development and progression of osteoarthritis by affecting the activity of NF- κ B p65. *Immunopharmacol Immunotoxicol*. 2021;43(6):713-723. doi:10.1080/08923973.2021.1970764
33. Giustarini G, Huppelschoten S. The hepatotoxic fluoroquinolone trovafloxacin disturbs TNF- and LPS-induced p65 nuclear translocation in vivo and in vitro. *Toxicol Appl Pharmacol*. 2020;391:114915